American Mineralogist, Volume 93, pages 1187–1190, 2008

LETTER

Modification of gas speciation in quartz-hosted fluid inclusions by stray laser radiation during LA-ICPMS analysis

GLENN LAMBRECHT, LARRYN W. DIAMOND,* AND THOMAS PETTKE

Rock-Water Interaction Group, Institute of Geological Sciences, University of Bern, Baltzerstrasse 3, CH-3012 Bern, Switzerland

ABSTRACT

Laser-ablation inductively coupled-plasma mass spectrometry (LA-ICPMS) is an established method of analyzing the elemental composition of individual fluid inclusions in minerals. While the method affords good spatial control of ablation pits, we have found that stray light from the UV (193 nm) laser may permanently modify the gas species in adjacent fluid inclusions. We have used Raman spectroscopy to analyze natural fluid inclusions in quartz before and after ablating test pits. New molecular species (CO, H_2, and O_2) appeared in the vapor phases of inclusions near the pits, resulting in complex, disequilibrium gas mixtures (e.g., CO_2-CH_4-H_2O-CO-H_2-O_2) and formation of iron oxyhydroxides in brine inclusions. Ablation for 40 s with a laser fluence of ~24 J/cm^2 on the sample produced the new gas species in inclusions at various distances up to 210 μm from the pits, depending on pit diameter. We attribute the changes in gas speciation to molecular photodissociation induced by stray UV-laser light. We have no evidence that this artifact changes the bulk elemental composition or density of the affected inclusions. The problem for fluid inclusion analysis is that phase-transition temperatures (e.g., clathrate hydrate dissociation, partial homogenization of the carbonic phases, and total homogenization) are highly sensitive to the mixture of gas species present. This means that parameters such as gas compositions, bulk salinity, and minimum entrapment temperatures are likely to be misinterpreted if inclusions are analyzed by microthermometry or Raman spectroscopy in samples that have already undergone laser ablation.

Keywords: Fluid inclusion, Raman spectroscopy, laser ablation ICP-MS, microthermometry, gas, speciation

INTRODUCTION

Laser-ablation inductively coupled-plasma mass spectrometry (LA-ICPMS) has become a popular tool to determine major and trace elements in individual fluid inclusions in minerals (Heinrich et al. 2003). The method is destructive but it offers unparalleled sensitivity and access to a huge range of detectable elements. Quantification of the results requires prior microthermometric determination of the bulk salinity of the inclusions. Although ablation with high-energy UV lasers affords exceptional spatial resolution, some side effects are known to occur outside the immediate volume of the ablated pits. For example, during analysis it is often observed that the vapor phase of inclusions close to the ablation spot is physically split into several bubbles. While the laser beam is on, the bubbles vibrate independently but when ablation stops the bubbles coalesce after a few minutes and the inclusion returns to its original state. Another example is the formation of specks and aggregates of fine-grained, brown solids in brine inclusions. These observations demonstrate that LA-ICPMS has some influence on inclusions in the vicinity of the ablation spot, but it is generally assumed that their composition remains unaltered. However, during routine analysis of aqueous inclusions in quartz we have found irreversible changes in the chemical speciation of the vapor phase in inclusions adjacent to the ablation pit. Failure to recognize such artifacts could lead to quite erroneous interpretations of the affected inclusions if they are investigated by microthermometry or Raman spectroscopy after an LA-ICPMS analytical session.

The purpose of this article is to describe these new observations and to alert fluid inclusion researchers to the problems that may arise. We report the results of simple experiments in which Raman spectroscopy was used to analyze the vapor phase of inclusions near ablation pits, before and after laser ablation. The results provide insight into the cause of the modifications and a first-order estimate of their spatial extent.

SAMPLES FOR ANALYSIS

The samples used in this study are hydrothermal quartz crystals from an orogenic gold deposit at Brusson, northwest Italian Alps (Diamond 1990), and from a porphyry Cu-Au deposit at Rosia Poieni, Romania (e.g., Kouzmanov et al. 2004; Milu et al. 2004). The crystals were cut along the *c* axis and prepared as doubly polished sections of about 1 mm thickness. Three compositional types of fluid inclusions were analyzed. First, low-X_{CO_2} carbonic inclusions from the Brusson locality, as previously described by Diamond (1990). At room temperature these

---

* E-mail: diamond@geo.unibe.ch

0003-004X/08/0007–1187$05.00/DOI: 10.2138/am.2008.2960

contain three fluid phases: a weakly saline aqueous liquid (4.5 to 6 mass% NaCl equiv.), carbonic liquid, and carbonic vapor. The combined carbonic phases occupy about 15 to 20 vol% of the inclusions, and in addition to CO_2 they have minor amounts of N_2 and CH_4. Second, aqueous inclusions from the Brusson locality, previously not described in the literature of this field area. At room temperature, they consist of saline aqueous liquid and around 10 to 15 vol% vapor, the latter being a mixture of CH_4, CO_2, N_2, and H_2O. Third, hypersaline brine inclusions from the Rosia Poieni locality, previously described briefly by Pettke et al. (2001). At room temperature, they consist of a CO_2-bearing vapor bubble, aqueous liquid, and daughter crystals of halite, sylvite, hematite, pyrite, chalcopyrite, and at least one other transparent mineral. Their bulk salinity is about 60 mass% NaCl equiv. as determined by microthermometry.

EXPERIMENTAL METHODS

Raman spectroscopy was performed with a Jobin Yvon LabRAM-HR800 instrument, an integrated Raman microprobe consisting of an Olympus BX41 confocal microscope coupled to an 800 mm focal-length spectrograph. A frequency-doubled Nd-YAG continuous-wave laser with an excitation wavelength of 532.12 nm (green) and a sample power of about 19 mW was focused on the vapor bubble of the target inclusion and the Raman signal was collected in backscattered mode. The sampled volume was a few μm^3 using a 100× objective. Acquisition time for most measurements was 2 × 120 s. Acquisitions of 3 × 240 s were used when higher sensitivity was needed. The spectra were recorded with the software Labspec v. 4.14.

The laser system used is a GeoLasPRO 193 nm ArF pulsed excimer laser, the latest commercial version of a prototype system developed at ETH, Zurich (Günther et al. 1997). This system allows the beam spot size to be set between 4 and 160 µm diameter with a uniform fluence over the illuminated area. Observation of the sample is through a Schwarzschild lens by CCD camera and microscope with reflected and transmitted light.

Suitable fluid inclusion assemblages were selected and the various gas species in the vapor phases were identified at room temperature by Raman spectroscopy. A pit was ablated near each assemblage. Pits of 44, 60, 90, and 120 µm diameter were ablated with a laser fluence of about 24 J/cm^2 on the sample. This fluence is typical of routine LA-ICPMS analyses in quartz. A 60 µm pit, using a fluence of about 32 J/cm^2 was ablated to investigate the effect of higher laser energies. For each pit, a stepwise opening procedure with increasing laser spot size was used and ablation continued for about 40 s on the final spot. After ablation, the gas species in the vapor phases of the adjacent fluid inclusions were analyzed again at room temperature by Raman spectroscopy.

RESULTS

We recall that, prior to laser ablation, the weakly saline aqueous and carbonic inclusions contained molecular CH_4, CO_2, H_2O, and N_2, and the brine inclusions contained molecular CO_2 and H_2O. After laser ablation, the aqueous and carbonic inclusions near ablation pits contained molecular CO, H_2, and O_2 in addition to their original gas species. The brine inclusions contained additional molecular H_2 only (Fig. 1). The intensity of the Raman bands of CO, H_2, and O_2 decreased in inclusions at greater distances from the pit. The Raman band of H_2 appeared more intense in the CO_2-poor aqueous inclusions and in the brine inclusions. Similar gas mixtures containing CH_4, CO_2, CO, N_2, H_2, H_2O, and O_2 were also detected in samples that had undergone laser ablation more than half a year before.

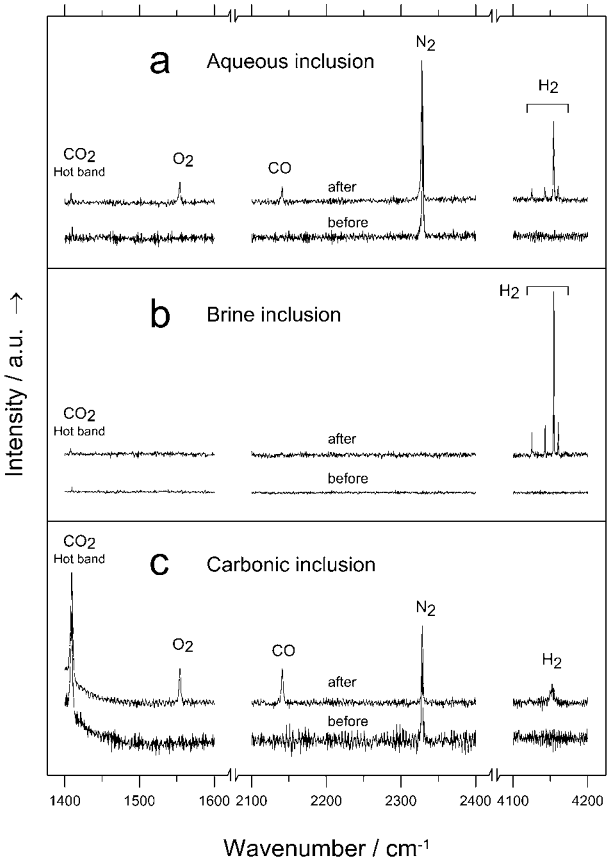

FIGURE 1. Raman spectra of (**a**) an aqueous inclusion, (**b**) a brine inclusion, and (**c**) a carbonic inclusion, before (lower spectra) and after (upper spectra) laser ablation of a nearby pit. To aid comparison, the spectra are normalized to the intensity (in arbitrary units, a.u.) of the minor "hot band" of CO_2 at ~1410 cm^{-1}. The spectra of the brine inclusion are corrected for background (atmospheric) gases. All spectra are baseline corrected.

After laser ablation, the aqueous and carbonic inclusions had not changed their appearance. In the brine inclusions, however, aggregates and specks of fine-grained, yellowish-brown solids appeared (Fig. 2). The Raman spectra of these new solids are very similar to that of goethite, but they could be any of several similar iron oxyhydroxides. In addition to the new solids, some of the brine inclusions near the ablation pit display corroded and irregular outlines (white arrow in Fig. 2b).

Table 1 shows the maximum and minimum distances from the ablation pit at which modified and unmodified inclusions could be found. Distances were measured from the central axis of the ablation pit to the edge of the inclusion while focusing on the inclusion through a normal petrographic microscope. The samples do not contain dense clusters of inclusions and so the spatial extent of the gas modification is not precisely defined. Nevertheless, for each investigated pit size and laser fluence, we have estimated a "modification" distance, i.e., a distance within which modifications of the gas speciation can be observed. For the experiments using a fluence of about 24 J/cm^2 on the sample, the "modification" distance is 110, 150, 210, and 210 µm for pits with diameters of 44, 60, 90, and 120 µm, respectively. For the experiment in which a higher energy density of 32 J/cm^2 and a 60 µm pit size was used, the "modification" distance is 150 µm. Inclusions located below ablation pits were also found to be modified.

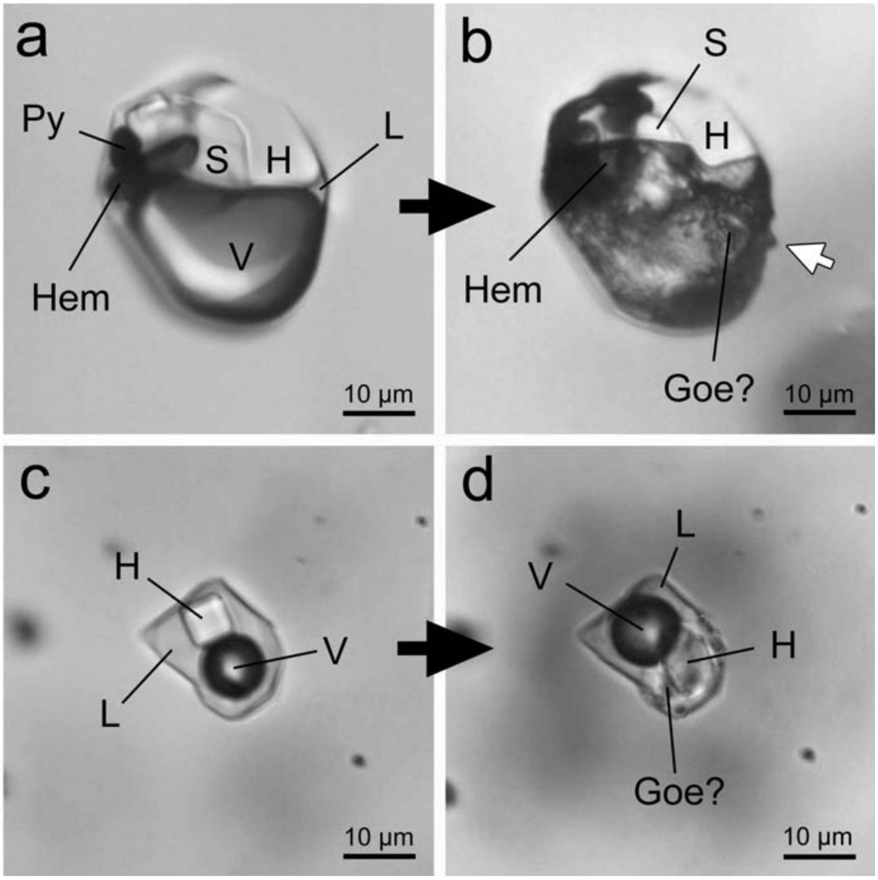

FIGURE 2. Transmitted-light photomicrographs of two brine inclusions before (**a**, **c**) and after (**b**, **d**) laser ablation of a nearby pit. Phases labeled are vapor (V), liquid (L), halite (H), sylvite (S), hematite (Hem), pyrite (Py), and goethite-like Fe-oxyhydroxide (Goe?). The dark shadow at the bottom right of **b** and the shadows around the inclusion in **d** are ablation pits out of focus.

TABLE 1. Results of laser ablation experiments

Ablation pit diameter (μm)	Laser fluence on sample (J/cm^2)	Maximum distance of modified fluid inclusion (μm)	Minimum distance of unmodified fluid inclusion (μm)	Estimated "modification" distance (μm)
44	24	88	108	110
60	24	98	145	150
60	32	135	105	150
90	24	158	205	210
120	24	193	208	210

DISCUSSION

The co-existence of measurable amounts of molecular CO, CO_2, CH_4, H_2, H_2O, and O_2 within individual vapor bubbles at room temperature implies chemical disequilibrium. Although this is in itself a strong indication of an artifact (it was this observation that first alerted us to the effect under discussion), co-existing molecular H_2 and O_2 have been reported previously in natural fluid inclusions from uranium ore bodies (Dubessy et al. 1988; Derome et al. 2003). These authors suggest that H_2 and O_2 resulted from the radiolysis of former H_2O molecules due to radioactive decay of nearby uranium minerals. In our samples, we assume that an analogous process of photodissociation is induced by the UV laser radiation that is incompletely absorbed by the host quartz. The dissociation of CO_2 and H_2O in the inclusions thus generates the species CO, H_2, and O_2:

$$2H_2O + h\nu \rightarrow 2H_2 + O_2$$
$$2CO_2 + h\nu \rightarrow 2CO + O_2$$

where $h\nu$ denotes 193 nm photons. These reactions may explain the higher intensity of the H_2 Raman band in the aqueous and brine inclusions (Fig. 1). The absence of molecular O_2 in the brine inclusions (Fig. 1b) is attributed to its immediate consumption via reaction with aqueous Fe-chloride to form the observed ferric oxyhydroxide solids (Fig. 2), e.g.:

$$0.25O_{2(g)} + 1.5H_2O_{(g)} + Fe^{2+}_{(aq)} \rightarrow FeO(OH)_{(s)} + 2H^+_{(aq)}$$

Some photolysis may also occur, but we have not detected any ionized molecular species by Raman spectroscopy. Since we have found H_2, CO, and O_2 in the vapor phases of samples that underwent laser ablation more than half a year before, it appears that the chemical modification is permanent. This is in accord with the long-term preservation of metastable molecular H_2 and O_2 within the natural fluid inclusions affected by radiolysis.

Laser-induced molecular photodissociation is well known in various fields of chemical physics (e.g., Schinke 1995). Although the absorption of 193 nm radiation by CO_2 and H_2O molecules is miniscule at room temperature (cross-section ~10^{-22} cm^2), it rapidly increases at higher temperatures, promoting dissociation of the molecules (Schulz et al. 2002). Presumably, quartz beneath the laser ablation pit is heated by the laser pulses, thereby heating the fluid inclusions. The resulting rapid thermal fluctuations and associated shockwaves may be the cause of the commonly observed splitting and vibration of the gas bubbles.

The "modification" distances suggested in Table 1 give us an idea of the size of the volume in which the speciation within fluid inclusions may be altered by laser ablation. Note that, for the experiment with a fluence of 32 J/cm^2 on the sample, an unmodified inclusion was found closer to the ablation pit (105 µm) than one of the modified inclusions (135 µm). However, the latter was situated at a greater depth (150 µm) than the former (40 µm). This observation allows us to speculate on the shape of the affected volume (Fig. 3). We can imagine that the laser beam is diffracted through a range of angles θ when it hits the imperfectly polished sample surface. This would create an inverted cone-shaped volume in which modification of fluid inclusions occurs. Thus, an inclusion that is located close to the ablation pit at shallow depth could lie above this cone, while other inclusions further from the pit and deeper in the sample are affected. From our experiments, it was not possible to determine whether the modified volume was symmetric around the central axis of the ablation pit.

We have found no evidence that the elemental composition of the fluid inclusions changes upon peripheral irradiation by the 193 nm laser, and no evidence that material leaks from the inclusions during or after ablation. We therefore assume that the bulk composition and the bulk density (or molar volume) of the inclusions remain constant. Nevertheless, the change in speciation of the gases has an important impact on microthermometric measurements of phase transitions. The dissociation temperature of gas clathrate hydrates, from which salinity is usually calculated in gas-bearing inclusions, is strongly dependent on the gas speciation (Diamond 1994). Similarly, the homogenization temperatures of the carbonic phases and of the total inclusion also depend on the mixture of volatile species present (Diamond 2003). In particular, the shift in total homogenization temperature would invalidate its use as a minimum constraint on the fluid entrapment temperature.

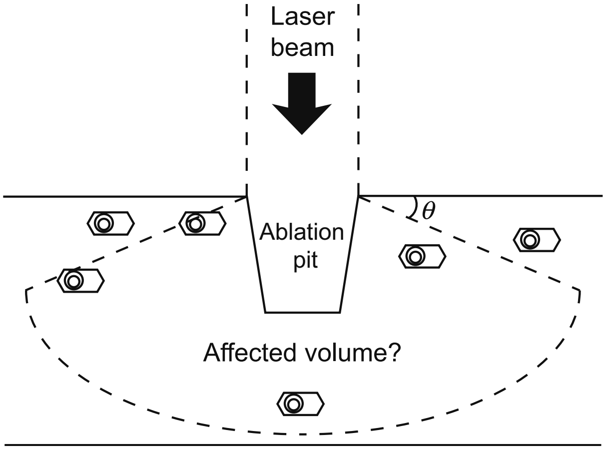

FIGURE 3. Conceptual sketch (not to scale) of the cone-shaped volume around an ablation pit in which modified fluid inclusions can be found. Note how the top left inclusion is located outside the affected volume, although it is closer to the ablation pit than the leftmost inclusion.

In view of the misinterpretations that could arise, we advise researchers to avoid conducting, or at least be careful when conducting, microthermometry or Raman analysis on fluid inclusions in samples that have already undergone laser ablation analysis. Table 1 can be used as a rough estimate of the volume in which fluid inclusions may be modified by photodissociation around a UV-laser ablation pit.

ACKNOWLEDGMENTS

We thank Alexandre Tarantola, Carl Spandler, and János Kodolányi of the Institute of Geological Sciences at Bern for stimulating discussions. The fluid inclusion and LA-ICPMS laboratories at Bern are supported by Swiss National Science Foundation Grants 200020-111834 to L.W. Diamond and PP002-106569 to T. Pettke.

REFERENCES CITED

Derome, D., Cathelineau, M., Lhomme, T., and Cuney, M. (2003) Fluid inclusion evidence of the differential migration of H_2 and O_2 in the McArthur River unconformity-type uranium deposit (Saskatchewan, Canada). Possible role on post-ore modifications of the host rocks. Journal of Geochemical Exploration, 78–79, 525–530.

Diamond, L.W. (1990) Fluid inclusion evidence for *P-V-T-X* evolution of hydrothermal solutions in late-alpine gold-quartz veins at Brusson, Val d'Ayas, northwest Italian Alps. American Journal of Science, 290, 912–958.

——— (1994) Salinity of multivolatile fluid inclusions determined from clathrate hydrate stability. Geochimica et Cosmochimica Acta, 58, 19–41.

——— (2003) Introduction to gas-bearing aqueous fluid inclusions. In I. Samson, A.J. Anderson, and D.M. Marshall, Eds., Fluid Inclusions: Analysis and Interpretation, 32, p. 101–158. Mineralogical Association of Canada, Quebec.

Dubessy, J., Pagel, M., Beny, J.-M., Christensen, H., Hickel, B., Kosztolanyi, C., and Poty, B. (1988) Radiolysis evidenced by H_2-O_2 and H_2-bearing fluid inclusions in three uranium deposits. Geochimica et Cosmochimica Acta, 52, 1155–1167.

Günther, D., Frischknecht, R., Heinrich, C.A., and Kahlert, H.-J. (1997) Capabilities of an argon fluoride 193 nm excimer laser for laser ablation inductively coupled plasma mass spectrometry microanalysis of geological materials. Journal of Analytical Atomic Spectrometry, 12, 939–944.

Heinrich, C.A., Pettke, T., Halter, W.E., Aigner-Torres, M., Audétat, A., Günther, D., Hattendorf, B., Bleiner, D., Guillong, M., and Horn, I. (2003) Quantitative multi-element analysis of minerals, fluid and melt inclusions by laser-ablation inductively-coupled-plasma mass-spectrometry. Geochimica et Cosmochimica Acta, 67, 3473–3496.

Kouzmanov, K., Wallier, S., Rey, R., Pettke, T., Ivascanu, P., and Heinrich, C. (2004) High-sulfidation veining in the porphyry Cu-Au deposit of Rosia Poieni, Romania: Fluid processes at the porphyry-to-epithermal transition. Annual Meeting of the Society of Economic Geology, Perth, Australia.

Milu, V., Milesi, J.-P., and Leroy, J.L. (2004) Rosia Poieni copper deposit, Apuseni Mountains, Romania: Advanced argillic overprint of a porphyry system. Mineralium Deposita, 39, 173–188.

Pettke, T., Halter, W.E., Driesner, T., von Quadt, A., and Heinrich, C.A. (2001) The porphyry to epithermal link: Preliminary fluid chemical results from the Apunseni Mountains, Romania, and Famatina, Argentinian Andes. Eleventh Annual V.M. Goldschmidt Conference, Hot Springs, Virginia.

Schinke, R. (1995) Photodissociation Dynamics: Spectroscopy and Fragmentation of Small Polyatomic Molecules. Cambridge Monographs on Atomic, Molecular and Chemical Physics, 1, 433 p. Cambridge University Press, New York.

Schulz, C., Koch, J.D., Davidson, D.F., Jeffries, J.B., and Hanson, R.K. (2002) Ultraviolet absorption spectra of shock-heated carbon dioxide and water between 900 and 3050 K. Chemical Physics Letters, 355, 82–88.

MANUSCRIPT RECEIVED FEBRUARY 20, 2008
MANUSCRIPT ACCEPTED FEBRUARY 28, 2008
MANUSCRIPT HANDLED BY BRYAN CHAKOUMAKOS